Journal Pre-proof

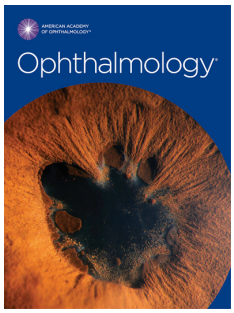

X-linked Retinoschisis: Deep Phenotyping and Genetic Characterization

Michalis Georgiou, MD, PhD, Lucia Finocchio, MD, Kaoru Fujinami, PhD, Yu Fujinami-Yokokawa, MPH, Gianni Virgili, MD, Omar A. Mahroo, PhD, FRCOphth, Andrew R. Webster, MD(Res), FRCOphth, Michel Michaelides, MD(Res), FRCOphth

PII: S0161-6420(21)00911-8

DOI: https://doi.org/10.1016/j.ophtha.2021.11.019

Reference: OPHTHA 11915

To appear in: *Ophthalmology*

Received Date: 16 September 2021

Revised Date: 4 November 2021

Accepted Date: 9 November 2021

Please cite this article as: Georgiou M, Finocchio L, Fujinami K, Fujinami-Yokokawa Y, Virgili G, Mahroo OA, Webster AR, Michaelides M, X-linked Retinoschisis: Deep Phenotyping and Genetic Characterization, *Ophthalmology* (2021), doi: https://doi.org/10.1016/j.ophtha.2021.11.019.

X-linked Retinoschisis: Deep Phenotyping and Genetic Characterization

Michalis Georgiou, MD, PhD,[1, 2, 3†] michalis.georgiou.16@ucl.ac.uk
Lucia Finocchio, MD, [1, 4†] luciafinocchio@gmail.com
Kaoru Fujinami, PhD,[1, 2, 5†] k.fujinami@ucl.ac.uk
Yu Fujinami-Yokokawa, MPH,[5, 6] y.fujinami@keio.jp
Gianni Virgili, MD,[4,7] gianni.virgili@unifi.it
Omar A. Mahroo, PhD, FRCOphth,[1,2] o.mahroo@ucl.ac.uk
Andrew R. Webster, MD(Res), FRCOphth,[1, 2] andrew.webster@ucl.ac.uk
Michel Michaelides, MD(Res), FRCOphth[1, 2] * michel.michaelides@ucl.ac.uk

[1] Moorfields Eye Hospital, London, United Kingdom.
[2] UCL Institute of Ophthalmology, University College London, London, United Kingdom.
[3] Jones Eye Institute, University of Arkansas for Medical Sciences, Little Rock, AR, USA.
[4] Department of Neuroscience, Psychology, Drug Research and Child Health, Ophthalmology, University of Florence-Careggi, Florence, Italy.
[5] Laboratory of Visual Physiology, Division of Vision Research, National Institute of Sensory Organs, National Hospital Organization Tokyo Medical Center, Tokyo, Japan.
[6] Department of Health Policy and Management, School of Medicine, Keio University, Tokyo, Japan.
[7]Centre for Public Health, Queen's University Belfast (Northern Ireland, UK)

†*Contributed equally and should be considered equivalent authors*
.

***Corresponding Author:**
Professor Michel Michaelides
UCL Institute of Ophthalmology
11-43 Bath Street
London, EC1V 9EL, UK
michel.michaelides@ucl.ac.uk

Financial Support: Supported by grants from the National Institute for Health Research Biomedical Research Centre at Moorfields Eye Hospital NHS Foundation Trust and UCL Institute of Ophthalmology, Onassis Foundation, Leventis Foundation, The Wellcome Trust (099173/Z/12/Z and 206619/Z/17/Z), Moorfields Eye Charity, Retina UK, and the Foundation Fighting Blindness (USA).

Financial Disclosures: Michalis Georgiou and Michel Michaelides consult for MeiraGTx

No conflicting relationship exists for any author.

Acknowledgements:

We thank Dr Xiao Liu, MD, National Institute of Sensory Organs, National Hospital Organization Tokyo Medical Center, Tokyo, Japan and Dr Lizhu Yang, MD, PhD, Department of Ophthalmology, Keio University School of Medicine, Tokyo, Japan for their contribution to the in silico genetic analysis and figure creation.

Word Count: 3704 words

Number of Figures: 3

Number of Tables: 2

Supplementary Materials: 9 (8 tables, 1 figure)

Running Title: X-linked Retinoschisis Natural History

Keywords: X-linked retinoschisis, RS1, XLRS, gene therapy, Optical Coherence Tomography, Fundus Autofluorescence, genotype, phenotype.

ABSTRACT

Objective: To examine the genetic and clinical features in children and adults with XLRS.

Design: Single-center consecutive, retrospective, observational study.

Setting: Single tertiary referral center.

Participants: Adults and children, with molecularly confirmed XLRS, followed up between 1999 and 2020.

Main Outcomes and Measures:
Genetic, clinical and retinal imaging findings, including optical coherence tomography (OCT) and fundus autofluorescence (FAF), cross-sectionally and longitudinally; and explore correlations including between best corrected visual acuity (BCVA) and age, and OCT characteristics.

Results:
One hundred and thirty-two males were identified, harbouring 66 *RS1* variants, with seven being novel. The mean age of onset was 16.5 years (range 2 to 55 years). Seventy-one patients (71/75, 94.7%) were symptomatic at presentation; all had decreased BCVA. Fundoscopy findings were symmetric in 104 patients (104/108, 96.3%), with the most common finding being macular schisis (82.4%), whereas peripheral retinoschisis was present in 38.9% and macular atrophy in 11.1%. Twenty patients (18.5%) developed complications (vitreous haemorrhage and/or retinal detachment). Mean BCVA was 0.65 LogMAR (20/89 Snellen) in the right eye and 0.64 LogMAR (20/87 Snellen) in the left eye.

Mean BCVA change over a mean interval of 6.7 years was 0.04 and 0.01 LogMAR for right and left eyes, respectively. FAF was normal in 16 of 106 eyes (15.1%); 45 eyes (42.5%) showed a spoke-wheel pattern, 13 (12.3%) had foveal hyperautofluorescence, while 18 (17.0%) had central reduction in signal. In total, 14 patients had evidence of FAF progression over time, indicated by change in the FAF pattern. On OCT, foveoschisis was observed in 172 eyes (172/215, 80%), parafoveal schisis in 171 (171/215, 79.5%), and foveal atrophy in 44 (44/215, 20.5%). Cystoid changes were localized to the inner nuclear layer (172/181 eyes, 95%), the outer nuclear layer (97/181, 53.6%) and the ganglion cell layer (92/181, 50.8%). Null variants were associated with worse final BCVA and aforementioned complications.

Conclusions and Relevance:

XLRS is highly phenotypically variable but with relative foveal preservation (and associated BCVA) until late adulthood, allowing more accurate prognostication. The slowly (often minimally) progressive disease course may pose a challenge in identification of early endpoints for therapeutic trials aimed at altering kinetics of degeneration.

INTRODUCTION

X-linked retinoschisis (XLRS, MIM #312700) is the most frequent inherited retinal disease (IRD) presenting in young males, accounting for about 5% of all childhood-onset IRD, with an estimated prevalence of 1 in 15,000-30,000.[1, 2] It is caused by pathogenic variants in the retinoschisin 1 gene (*RS1*, OMIM # 300839).[3] Retinoschisin-1 protein is expressed in photoreceptors and bipolar cells, and has a role in retinal cell adhesion. *RS1* variants disrupt the subunit assembly of the protein and lead to alteration of normal retinal cell adhesion, thus resulting in splitting of the neural layers of the retina.[2]

XLRS typically presents in the first to second decade with variable manifestations, including poor visual acuity, strabismus, anisometropia and 'unexplained visual loss', but a smaller number of patients present in infancy with strabismus, nystagmus and/or bullous retinoschisis.[2] Macular examination can reveal the typical 'spoke-wheel' folds (macular schisis), fine white dots resembling drusen-like deposits, non-specific retinal pigment epithelial (RPE) changes and macular atrophy, with the latter being seen in older individuals.[4, 5] During the disease course, secondary complications including vitreous or intraschisis haemorrhage, retinal neovascularization, subretinal exudation, retinal detachment (RD) and traumatic rupture of foveal schisis can occur. Approximately 50% of patients also have peripheral retinal changes, including schisis, metallic sheen, pigmentary disturbance, white spiculations, vitreous veils and neovascularization.[5, 6] Natural history and prognosis are not well established and have been mostly explored in small cohorts, with limited follow-up.

Using optical coherence tomography (OCT) foveoschisis has been reported in 78-81% of patients with XLRS and an isolated parafoveal schisis in a further 10%.[7, 8] Schisis cavities can be found in any retinal layer; retinal nerve fiber layer (RNFL), ganglion cell layer (GCL), inner nuclear layer (INL), outer plexiform layer (OPL) and outer nuclear layer

(ONL).[9] Nevertheless, intraretinal cysts are found predominantly in the INL, followed by the OPL and GCL.[10] It is unclear what the implications are of the pattern or location of these cavities. Qualitative changes are also seen in the interdigitation zone (IZ), ellipsoid zone (EZ), external limiting membrane and photoreceptor outer segments.[4] An increased inner retinal foveal thickness and decreased perifoveal inner retinal thickness have been reported to correlate with worse visual acuity.[8] A spoke-wheel pattern of high and low intensity signal represents the characteristic fundus autofluorescence (FAF) findings in XLRS, due to displacement of luteal pigment.[4] Nevertheless, recently it has been identified in only approximately half of patients.[6, 7] Normal FAF, low signal in the foveal region, an area of low signal surrounded by a ring of increased signal intensity, or irregular or regular concentric areas of high- and low-intensity FAF can also be observed.[4]

It is imperative to understand the natural progression of the disease and to perform a precise phenotypic characterization when choosing outcome measures to monitor disease progression and outcomes of therapeutic interventions. Herein we examined the clinical characteristics, the structural and functional outcomes in the largest single center XLRS cohort reported in the literature, consisting of 132 molecularly confirmed children and adults. We describe their genetic and clinical features, investigate genotype-phenotype correlations, and establish longitudinal clinical correlations between best-corrected visual acuity (BCVA) and age, OCT characteristics, FAF features, and complications.

MATERIALS AND METHODS

The study adhered to the tenets of the Declaration of Helsinki. Each subject (and a parent of children <18 years of age) gave written informed consent before genetic testing. Ethical approval was obtained from Moorfields Eye Hospital (MEH, London, UK) for this retrospective single-center observational series.

Subjects

Adults and children with XLRS, examined in the retinal genetics service in a single tertiary center (MEH, London, UK), were recruited. XLRS diagnosis was based on clinical findings, family history and confirmed by detection of a disease-causing *RS1* variant.

RS1 Genetic Analysis

A combination of direct Sanger sequencing and next generation sequencing, including panels of retinal dystrophy genes, whole exome sequencing (WES) and whole genome sequencing (WGS), was used to identify variants in the *RS1* gene. All recruited patients were reassessed for their detected *RS1* variants, as described in **Supplementary Material - Methods**.

Ocular Examination and Retinal Imaging

Review of clinical records, including medical and ocular histories, slit-lamp biomicroscopy, and a dilated funduscopic examination was performed. Age of onset was defined as the age of the first reported symptoms. BCVA was measured using the Snellen charts and converted into logarithm of the minimum angle of resolution (LogMAR) units for statistical analysis. Fundus photography (Optos ultra widefield camera, Optos, Scotland, UK), infrared reflectance (IR), spectral domain (SD) -OCT (Spectralis OCT, Heidelberg Engineering, Dossenheim, Germany) and short-wavelength (488-nm) FAF were performed

longitudinally for most of the patients. Analysis was performed using all available data. Not all modalities/tests were always available at the same, different baseline and last follow-up was used to maximize follow-up time for all the studied parameters. The mean age and follow-up time are reported individually for each parameter. The presence of complications, such as vitreous haemorrhage (VH) or RD were evaluated.

Fundus Autofluorescence

Spectralis OCT was used to obtain high resolution FAF images. The data were registered at baseline and at the last follow-up. We identified four patterns and patients were assigned to each group: i) spoke-wheel pattern, ii) increased central signal, iii) central reduction in signal, and iv) ring of increased signal (**Figure 1**).

Optical Coherence Tomography

SD-OCT was used to obtain high resolution horizontal line scans of the macula in both eyes of the participants. The data were registered at baseline and at the last follow-up. The presence of foveoschisis, parafoveal schisis and foveal atrophy was evaluated. Schisis localization using vertical and horizontal central macular OCT images was analyzed by evaluating RNFL, GCL, INL, OPL, inner plexiform layer (IPL) and ONL. Central macular thickness (CMT) was calculated automatically using a circular ETDRS-type grid positioned on the center of the fovea (central circle of approximately 1-mm diameter), after the scans were reviewed and corrected manually if needed. Defects in the outer retinal photoreceptor microstructures were evaluated, including the IZ and EZ in an area 1 mm from the foveal center, also using vertical and horizontal central OCT images. An IZ defect was defined as an irregularity or definite defect of the line. Disruptions in the EZ were defined as signal interruptions at the level of the EZ line. Foveal atrophy was defined as total absence of the IZ or EZ bands. The photoreceptor outer segment (PROS)

thickness was calculated by manual measurement of the distance between the EZ and the anterior surface of the retinal pigment epithelium (RPE), as described previously.[11] The presence of specific OCT findings, including schisis and defects, was determined by consensus between two observers (LF and MG). Any discrepancies between the observers were resolved through discussion with the principal investigator (MM), until consensus was reached.

Statistical Analysis

Statistical analysis was carried out using SPSS Statistics for Windows (Version 22.0. Armonk, NY: IBM Corp.). Significance for all statistical tests was set at $P<0.05$. The Shapiro-Wilk test was used to test for normality for all variables.

RESULTS

Demographic data

We ascertained 132 males, from 126 families, followed up between 1999 and 2020. Clinical data and BCVA, were available at one or more visit for 127 patients. The mean age (±SD, range) of the group was 25.4 years (±16.7, 2.3-70.8 years). The baseline age and the follow-up time is indicated below for each assessment.

RS1 Genetic Analysis

All recruited patients had pathogenic or likely pathogenic variants in *RS1*. In total 66 variants were identified. **Table 1** presents the 12 most prevalent variants, and **Figure 2** presents the localization of the identified variants in the gene domains. The five most prevalent variants account for 30.2% of affected families. Seven variants are novel (**Table 1**). One variant (c.52+5G>C) was identified in cis with the variant c.35T>A, in three patients, from three different pedigrees, and based on *in silico* analysis may not contribute to disease. **Supplementary Table 1**, presents all sequence variants, based on their HGVS nomenclature and their predicted effect. Missense variants were the most common type of alteration (n=48, 72.7%). Pathogenicity assessment based on the ACMG guidelines, allele frequency, coverage, general and functional prediction scores, and conservation scores of all detected variants are presented in **Supplementary Tables 2-6. Supplemental Figure 1** presents evolutionary conservation for detected missense variants.

Disease Onset

Age of onset was recorded in years for 61 patients. The mean (±SD, range, median) age of onset was 16.5 years (±15.4, 0-58, 11 years). One patient (1.3%) showed symptoms shortly after birth. Half of the patients were symptomatic before the age of 11. Age at

baseline examination is detailed in the BCVA section. **Table 2** summarizes the age of onset and all clinical findings. **Figure 3A** presents the age of onset by age group for the cohort.

Signs and Symptoms

Signs and symptoms were available for 75 patients. 71 (94.7%) were symptomatic at presentation. 4 were asymptomatic at first evaluation and were referred due to family history of XLRS. A universal finding was reported decreased VA (100%). The clinical presentation varied (**Table 2**) but symptoms included nyctalopia (n=6, 8.5%), strabismus (n=6, 8.5%), VH (n=3, 4.3%, bilateral in 1 case), RD (n=2, 2.7%), and nystagmus (n=1, 1.4%). No patient presented with photophobia or reduced color vision.

Fundoscopy findings were documented for 108 patients. Four had normal fundi. Findings were bilateral in 104 (96.3%). The most common finding was macular schisis (89 patients, 82.4%), whereas peripheral retinoschisis was present in 42 (38.9%). Atrophic macular thinning was present in 12 (11.1%). Only one patient had signs of macular atrophy and schisis. The mean age (range) of patients with macular atrophy was 46.5 years (19-66 years). In contrast, patients with foveal schisis were younger (mean, range: 22.1, 3-56 years). Twenty (18.5%) developed complications: 8 patients had VH (7.2%), 6 patients had VH and RD (5.6%), and 8 patients had RD without VH (7.2%).

Visual Acuity

BCVA was assessed cross-sectionally and longitudinally. 127 patients had BCVA available at one or more visits. None had any other vision limiting disease. Mean (±SD, range) age at baseline was 25.4 years (±16.7, 2.3 to 70.8 years). Mean BCVA (Snellen equivalent, ±SD, range LgMAR) was 0.65 LogMAR (89/20 Snellen, ±0.43, -0.1 to 3.0 LogMAR) for the right eye and 0.64 LogMAR (87/20 Snellen, ±0.44, 0.0 to 3.0 LogMAR) for the left eye at

baseline. Baseline BCVA was highly variable among patients, but there was no significant interocular difference (z=0.27, p=0.79, Wilcoxon Sign Rank test). There was a moderate statistically significant correlation between mean BCVA for right and left eyes, and the baseline age (r=0.39, P<0.01, Spearman's correlation coefficient). **Figure 3B**, presents the mean BCVA against age for the cohort. The moderate correlation may reflect the early severe decrease in BCVA and the further slow decline with age.

One hundred and thirteen patients had available longitudinal BCVA data. Mean (±SD, range) follow-up was 6.7 years (±5.2, 0.2-19.6 years). The mean BCVA (Snellen equivalent, ±SD, range LogMAR) was 0.69 LogMAR (20/98 Snellen, ±0.56, -0.10 to 3.0 LogMAR) and 0.65 LogMAR (20/89 Snellen, ±0.48, 0.0 to 3.0 LogMAR) for the right and left eyes respectively at last follow-up. The mean change over follow-up was 0.04 and 0.01 LogMAR for right and left eyes respectively, without significant interocular difference (p=0.38, z=0.88, Wilcoxon Sign Rank test). There was no significant correlation between mean rate of BCVA change for right and left eyes, and the baseline age (r=0.15, P=0.12, Spearman's correlation coefficient).

Fundus Autofluorescence

FAF was available for 108 patients for cross-sectional assessment (mean age ±SD: 27.7 ±16.1 years). Ten patients had low quality imaging in one eye and two patients for both eyes, that were excluded from analysis. In the remaining 96 patients, FAF pattern was similar bilaterally. For cross-sectional assessment the right eye was included from each patient (106 eyes from 106 patients).

Normal FAF was seen in 16 of 106 eyes (15.1%); 45 eyes (42.5%) showed a spoke-wheel pattern, 13 eyes (12.3%) showed foveal hyperautofluorescence ("increased central signal" pattern), while 18 eyes (17.0%) showed a "central reduction in signal". Central hypoautofluorescence surrounded by hyperautofluorescent borders ("ring of increased signal") was found in 14 eyes (13.2%): it was isolated in 7 eyes (6.6%), while it

was associated with spoke-wheel in 3 eyes (2.8%) and with central reduction in signal in 4 eyes (3.8%). The FAF findings at baseline are summarized in **Supplementary Table 7**.

Transition between patterns of FAF was highly variable, with no definite sequence. Progression from normal FAF to an “increased central signal” was observed in 2 eyes after a mean follow-up of 3 years, to “central reduction in signal” in 1 eye after 11 years, to “ring of increased signal” in 2 eyes after a mean follow-up of 3.5 ± 0.7 years. A progression from “spoke-wheel” to central reduction in signal was detected in 5 eyes after 6 ± 4.8 years, to “increased central signal” in 1 eye after 6 years, to “ring of increased signal” in 1 eye after 10 years, and to normal FAF in 3 eyes after a mean of 3.3 ± 3.2 years. Progression from “increased central signal” to normal was observed in 1 eye after 3 years and to “spoke-wheel” pattern in 1 eye after 5 years.

Optical Coherence Tomography

SD-OCT data were available for 215 eyes of 115 patients at baseline (mean age ±SD: 27.7 ±17.4 years). Foveoschisis was observed in 172 of 215 eyes (80%), parafoveal schisis in 171 of 215 eyes (79.5%), and foveal atrophy in 44 of 215 eyes (20.5%). The localization of the cavities was mapped for 181 eyes at baseline: localized mainly in the INL (172/181 eyes, 95%); and then in the ONL (97 eyes, 53.6%) and GCL (92 eyes, 50.8%). Cavities were observed in the OPL in 41 eyes (22.7%), and IPL in only 1 eye (0.6%). RNFL was involved in 2 eyes (1.1%). The mean CMT was 378.15 ± 162.13 µm (range, 46-1099 µm).

Qualitative analysis of photoreceptor structure at baseline revealed that the IZ was the most frequently affected and found to be disrupted in 139/220 eyes (63.2%). EZ analysis was possible in 218 eyes: it was disrupted in 133 eyes (61%). Mean PROS length was 36.9 ± 7.3 µm (range, 15-56 µm). Previously reported mean PROS length for healthy

individuals is 47±4 µm (range, 37–54 µm).[10] All OCT findings at baseline are summarized in **Supplementary Table 8**.

Follow-up OCT imaging was available for 187 eyes of 115 patients (mean age ±SD: 30.5 ±17.3 years). Foveoschisis was observed in 140 of 187 eyes (74.9%), parafoveal schisis in 129 eyes (68.9%) and foveal atrophy in 41 eyes (21.9%). Data on cavities were available for 175 eyes: localized mainly in the INL (164 /175, 93.7%); and then in the ONL (96 eyes, 54.9%) and GCL (85 eyes, 48.6%). Cavities were observed in the OPL in 34 eyes (19.4%). The mean CMT was 348.87 ± 164.15 µm (range, 28-1130 µm). No cavities were detected in the IPL and RNFL.

Qualitative analysis was performed at the last follow-up, with again the most frequently affected structure being the IZ, with IZ disruption in 119/183 eyes (65%). EZ analysis was possible in 184 eyes: it was disrupted in 118 eyes (64.1%). Mean PROS length was 36.38 ± 6.89 µm (range, 22-53 µm) and was similar to baseline (paired t-test).

Genotype-Phenotype correlations

The mean (±SD, range) age of onset for patients with null and missense variants was 18.3 years old (±15.6, 3-58) and 16.1 years old (±15.2, 0-55) respectively, and it was similar between the two groups (p=0.44, z=0.78, Mann-Whitney U). BCVA at last follow up was worse for patient with null variants (mean ±SD, range; 0.80 ±0.49, 0-2.1 LogMAR), compared to patients with missense variants (mean ±SD, range; 0.63 ±0.41, 0-2.2 LogMAR), however the difference was not statistically significant (p=0.07, z=1.81, Mann-Whitney U). From the 22 patients who developed complications (RD and/or VH), seven were harboring null variants and 15 had missense variants. The frequency of complications is similar among the two groups (p=0.09, x^2=2.83 chi-square).

DISCUSSION

The current study describes the genetic, clinical and imaging characteristics of 132 males from 126 families with molecularly confirmed XLRS, both cross-sectionally and longitudinally. It represents the largest cohort to date to undergo detailed analysis, including multimodal imaging and genotype-phenotype investigation. Our results provide insights into the retinal phenotype and natural history, over a wide range of ages.

Genotypic and Phenotypic Variability

Over 200 disease-associated variants in *RS1* are known, with most occurring as non-synonymous changes in the major protein unit (discoidin domain, Figure 2). In our study, 66 variants were identified, of which seven were novel. Missense variants were the most common (72.7%), in agreement with previous reports.[12] Phenotypic variability is documented in the literature, with a variety of factors thought to contribute, including the underlying variant and age.[13-17] Other studies report intrafamilial variability and lack of correlation between the type of variant and disease severity or progression.[12, 18-20] The most established correlation between genotype and phenotype has been described for ERG findings, where patients with null variants had consistently more severe ERG findings.[6, 13] The patients in our cohort showed profound phenotypic variability. Age of onset, BCVA at last follow-up and frequency of complications, were not statistically significantly different in our cohort, among patients with null and missense variants. However, it should be noted that the BCVA and frequency of complications had an association with the group with null variants (p=0.07 and p=0.09 respectively), and final BCVA was on average 0.27 LogMAR higher (worse BCVA), in the null variant group.

The clinical characteristics of our cohort are broadly in keeping with published reports. The most common retinal finding was macular schisis (n=89/108, 82.4%), whereas peripheral retinoschisis was present in more than one third of patients (n=42/108,

38.9%). Previous reports identified macular schisis from 68%-76% of patients, peripheral retinoschisis in 43%-60% and macular atrophy in 8%-10%.[5, 16, 21] Macular atrophy was present in 12 patients (11.1%), and only one patient had simultaneous findings of macular atrophy and schisis. Some studies have reported macular atrophy in patients in their fourth decade, and clinical descriptions of macular schisis flattening with age without a clear mechanism for these changes.[14, 22] In our study, we found the mean age (range) of patients with macular atrophy was 46.5 years (19-66 years). In contrast, patients with foveal schisis were younger (mean, range: 22.1, 3-56 years).

Twenty-two patients (19.8%) developed complications, such as VH and/or RD. The frequency of complications varies considerably in the literature, with a frequency between 3% to 21% for VH and 5% to 40% for RD.[5, 21, 23, 24] Recently we have reported increased incidence of VH and RD, in patients with peripheral schisis.[21] We can hypothesize that the natural history of XLRS often begins with a normal fundus in younger patients, then retinoschisis develops, with finally macular atrophy slowly developing at an older age; (which may be further complicated by VH and/or RD) - albeit with a significant age overlap in these aforementioned stages of disease progression.

BCVA varies widely, with previous studies reporting a mean BCVA of 0.49-0.6 LogMAR.[5, 10, 25] Mean BCVA in our study was 0.65 LogMAR and 0.64 LogMAR for the right and left eye respectively. Mean change over time was 0.04 and 0.01 LogMAR for right and left eyes respectively (mean follow-up 6.7 years), without significant interocular difference. These data indicate an overall relative stability, with very slow modest progression over time, in agreement with previous reports.[16, 26, 27] There was a moderate statistically significant correlation between mean BCVA for right and left eyes, and baseline age. The moderate correlation may reflect the early severe decrease in BCVA and further slow decline with age.

Structural Changes and Disease Natural History

FAF findings were highly variable including normal FAF, spoke-wheel pattern, foveal hyperautofluorescence and central reduction in signal. Hyperautofluorescent foveal borders ("ring of increased signal") was observed in isolation, or with central hypoautofluorescence, spoke-wheel, or central signal reduction. Variability in FAF has been reported.[6, 10] Spoke-wheel pattern, whilst characteristic in XLRS, was only identified in 42% of patients (45/106); with a recent report stating 54% (51/94 eyes).[7] We can speculate that there is progression (albeit not in all patients) from an increased central signal, to spoke-wheel pattern, and finally to central reduction in signal.

In keeping with the literature, foveoschisis was seen in 80% (172/215), parafoveal schisis in 79.5% (171/215), and foveal atrophy in 20.5% (44/215) of eyes.[10, 12] Foveal cavities occurred mostly in the INL (95%) and OPL(22.7%)/ONL(53.6%), and then GCL (50.8%).[8, 10, 28, 29] Our findings parallel, especially for INL, those reported by Andreoli et al*.* who found that schisis affected the INL and OPL, respectively, in 85% and 61% of cases;[8] and Orès et al*.* who identified schisis changes mainly in the INL (88%) and OPL (64%), followed by RNFL/GCL (46%) and ONL (22%).[10] In almost half of eyes, cavities were also found in the GCL in previous reports.[25, 29] None were detected in the IPL and RNFL. These data would be in keeping with the RS1 protein being widely distributed in the retinal layers. We provide further data to support that the most frequent qualitative defect in outer photoreceptor structure is disrupted IZ, identified in 63.2% of eyes at baseline and in 65% at last follow-up.[10] EZ disruption was observed in 61% at baseline and in 64% at last follow-up. The combined data to date support the hypothesis that the IZ defect may reflect the initial changes in photoreceptors; and that anatomical change over time is relatively limited.[25, 30]

Endpoints for Clinical trials

OCT measurements were the most widely available metric in the cohort, independently of disease state, and in agreement with a recent report, can provide metrics for clinical trials.[31] OCT measurements have been used as reliable endpoints in many IRD studies and trials .[32] OCT can also be used for the identification of early disease changes in retinal layers before the development of overt atrophy. However, the slow disease progression identified in our study may pose a challenge in quantification of changes in OCT that exceed the test-retest repeatability, within the time frame of a trial. Reliability and repeatability assessment studies, with standardized protocols should further evaluate the OCT metrics before employment in trials. FAF metrics such as area of atrophy, have also previously proven to have good repeatability in IRDs.[33] However, atrophy is only evident in a subset of patients with XLRS, and only in advanced disease, thereby limiting the utility of this modality in trials. Functional assessment beyond BCVA, such as microperimetry testing, as well as more advanced imaging techniques, such as adaptive optics imaging, [34] warrants further exploration in XLRS.

Future Directions

XLRS is an attractive target for gene therapy due to its monogenic nature and promising preclinical studies.[35] The *Rs1*-knockout mouse showed rapid structural and functional treatment benefit after intravitreal *RS1* gene replacement.[36, 37] Two phase I/II intravitreal gene therapy trials (NCT02416622 sponsored by Applied Genetics Technology Corp and NCT02317887 by the National Eye Institute) have been conducted: the former has been halted due to marked ocular inflammation, while the latter has added additional agents to the standard oral steroids used in subretinal gene supplementation trials to address the uveitis adverse events; further efficacy data are awaited.[38]

Limitations

The main limitations of our study are the retrospective design, the lack of a control group and the variable follow-up duration. An additional limitation is the lack of visual field data. Despite these limitations, this study provides a comprehensive analysis of the genetic, structural, and clinical characteristics of the largest XLRS cohort reported in the literature, with long-term follow up, helping to elucidate disease natural history.

Conclusions

XLRS has a wide spectrum of clinical characteristics, hence, molecular diagnosis is crucial for its early diagnosis and genetic counselling, as well as for potential participation in clinical trials. XLRS has a wide window of therapeutic opportunity, with most patients having relative preservation of foveal structure (and function) till the fourth decade of life. However, the disease has an early onset and often significantly reduced BCVA early in the disease course. The slow disease progression identified in our study may pose a challenge in the identification of early endpoints for interventions aiming to slow/halt degeneration.

LEGENDS

Figure 1: Fundus Autofluorescence Patterns in X-linked Retinoschisis.

Four main patterns were identified: **(A)** Spoke-wheel, **(B)** Increased central signal, **(C)** Central reduction in signal, and **(D)** Ring of increased signal.

Figure 2: Graphical representation of RS1.

RS1 consists of a signal peptide (amino acids (AA): 1-23, marked with grey), an Rs1 domain (AA: 23-62, marked with horizontal lines) and a discoidin domain (AA: 63-219, marked with diagonal lines). The identified variants in the current cohort are shown.

Figure 3: Age of Onset and Visual Acuity Graphs

(A) Age of onset by age group, with the vast majority having onset in childhood. **(B)** Presents the mean BCVA at baseline against age for 127 patients, showing a positive statistically significant correlation.

REFERENCES

1. Molday RS, Kellner U, Weber BH. X-linked juvenile retinoschisis: clinical diagnosis, genetic analysis, and molecular mechanisms. Prog Retin Eye Res 2012;31(3):195-212.
2. Rahman N, Georgiou M, Khan KN, Michaelides M. Macular dystrophies: clinical and imaging features, molecular genetics and therapeutic options. Br J Ophthalmol 2020;104(4):451-60.
3. Sauer CG, Gehrig A, Warneke-Wittstock R, et al. Positional cloning of the gene associated with X-linked juvenile retinoschisis. Nat Genet 1997;17(2):164-70.
4. De Silva SR, Arno G, Robson AG, et al. The X-linked retinopathies: Physiological insights, pathogenic mechanisms, phenotypic features and novel therapies. Prog Retin Eye Res 2020:100898.
5. George ND, Yates JR, Moore AT. Clinical features in affected males with X-linked retinoschisis. Arch Ophthalmol 1996;114(3):274-80.
6. Vincent A, Robson AG, Neveu MM, et al. A phenotype-genotype correlation study of X-linked retinoschisis. Ophthalmology 2013;120(7):1454-64.
7. Ores R, Mohand-Said S, Dhaenens CM, et al. Phenotypic Characteristics of a French Cohort of Patients with X-Linked Retinoschisis. Ophthalmology 2018;125(10):1587-96.
8. Andreoli MT, Lim JI. Optical coherence tomography retinal thickness and volume measurements in X-linked retinoschisis. Am J Ophthalmol 2014;158(3):567-73.e2.
9. Gregori NZ, Lam BL, Gregori G, et al. Wide-field spectral-domain optical coherence tomography in patients and carriers of X-linked retinoschisis. Ophthalmology 2013;120(1):169-74.
10. Orès R, Mohand-Said S, Dhaenens CM, et al. Phenotypic Characteristics of a French Cohort of Patients with X-Linked Retinoschisis. Ophthalmology 2018;125(10):1587-96.
11. Chen J, Xu K, Zhang X, et al. Novel mutations of the RS1 gene in a cohort of Chinese families with X-linked retinoschisis. Mol Vis 2014;20:132-9.
12. Gao FJ, Dong JH, Wang DD, et al. Comprehensive analysis of genetic and clinical characteristics of 30 patients with X-linked juvenile retinoschisis in China. Acta Ophthalmol 2020.
13. Bowles K, Cukras C, Turriff A, et al. X-linked retinoschisis: RS1 mutation severity and age affect the ERG phenotype in a cohort of 68 affected male subjects. Invest Ophthalmol Vis Sci 2011;52(12):9250-6.
14. Menke MN, Feke GT, Hirose T. Effect of aging on macular features of X-linked retinoschisis assessed with optical coherence tomography. Retina 2011;31(6):1186-92.
15. Lesch B, Szabó V, Kánya M, et al. Clinical and genetic findings in Hungarian patients with X-linked juvenile retinoschisis. Mol Vis 2008;14:2321-32.
16. Apushkin MA, Fishman GA, Rajagopalan AS. Fundus findings and longitudinal study of visual acuity loss in patients with X-linked retinoschisis. Retina 2005;25(5):612-8.
17. Chen C, Xie Y, Sun T, et al. Clinical findings and RS1 genotype in 90 Chinese families with X-linked retinoschisis. Mol Vis 2020;26:291-8.
18. Eksandh L, Andréasson S, Abrahamson M. Juvenile X-linked retinoschisis with normal scotopic b-wave in the electroretinogram at an early stage of the disease. Ophthalmic Genet 2005;26(3):111-7.
19. Pimenides D, George ND, Yates JR, et al. X-linked retinoschisis: clinical phenotype and RS1 genotype in 86 UK patients. J Med Genet 2005;42(6):e35.
20. Simonelli F, Cennamo G, Ziviello C, et al. Clinical features of X linked juvenile retinoschisis associated with new mutations in the XLRS1 gene in Italian families. Br J Ophthalmol 2003;87(9):1130-4.
21. Fahim AT, Ali N, Blachley T, Michaelides M. Peripheral fundus findings in X-linked retinoschisis. Br J Ophthalmol 2017;101(11):1555-9.
22. Genead MA, Fishman GA, Walia S. Efficacy of sustained topical dorzolamide therapy for cystic macular lesions in patients with X-linked retinoschisis. Arch Ophthalmol 2010;128(2):190-7.
23. Kellner U, Brümmer S, Foerster MH, Wessing A. X-linked congenital retinoschisis. Graefes Arch Clin Exp Ophthalmol 1990;228(5):432-7.

24. Roesch MT, Ewing CC, Gibson AE, Weber BH. The natural history of X-linked retinoschisis. Can J Ophthalmol 1998;33(3):149-58.
25. Yang HS, Lee JB, Yoon YH, Lee JY. Correlation between spectral-domain OCT findings and visual acuity in X-linked retinoschisis. Invest Ophthalmol Vis Sci 2014;55(5):3029-36.
26. Pennesi ME, Birch DG, Jayasundera KT, et al. Prospective Evaluation of Patients With X-Linked Retinoschisis During 18 Months. Invest Ophthalmol Vis Sci 2018;59(15):5941-56.
27. Cukras CA, Huryn LA, Jeffrey BG, et al. Analysis of Anatomic and Functional Measures in X-Linked Retinoschisis. Invest Ophthalmol Vis Sci 2018;59(7):2841-7.
28. Eriksson U, Larsson E, Holmström G. Optical coherence tomography in the diagnosis of juvenile X-linked retinoschisis. Acta Ophthalmol Scand 2004;82(2):218-23.
29. Gregori NZ, Berrocal AM, Gregori G, et al. Macular spectral-domain optical coherence tomography in patients with X linked retinoschisis. Br J Ophthalmol 2009;93(3):373-8.
30. Ling KP, Mangalesh S, Tran-Viet D, et al. Handheld spectral domain optical coherence tomography findings of x-linked retinoschisis in early childhood. Retina 2020;40(10):1996-2003.
31. Hahn LC, van Schooneveld MJ, Wesseling NL, et al. X-linked Retinoschisis: Novel Clinical Observations and Genetic Spectrum in 340 Patients. Ophthalmology 2021.
32. Daich Varela M, Esener B, Hashem SA, et al. Structural evaluation in inherited retinal diseases. Br J Ophthalmol 2021.
33. Georgiou M, Kane T, Tanna P, et al. Prospective Cohort Study of Childhood-Onset Stargardt Disease: Fundus Autofluorescence Imaging, Progression, Comparison with Adult-Onset Disease, and Disease Symmetry. Am J Ophthalmol 2019.
34. Georgiou M, Kalitzeos A, Patterson EJ, et al. Adaptive optics imaging of inherited retinal diseases. Br J Ophthalmol 2017.
35. Georgiou M, Fujinami K, Michaelides M. Inherited retinal diseases: Therapeutics, clinical trials and end points-A review. Clin Exp Ophthalmol 2021.
36. Ou J, Vijayasarathy C, Ziccardi L, et al. Synaptic pathology and therapeutic repair in adult retinoschisis mouse by AAV-RS1 transfer. J Clin Invest 2015;125(7):2891-903.
37. Byrne LC, Oztürk BE, Lee T, et al. Retinoschisin gene therapy in photoreceptors, Müller glia or all retinal cells in the Rs1h-/- mouse. Gene Ther 2014;21(6):585-92.
38. Cukras C, Wiley HE, Jeffrey BG, et al. Retinal AAV8-RS1 Gene Therapy for X-Linked Retinoschisis: Initial Findings from a Phase I/IIa Trial by Intravitreal Delivery. Mol Ther 2018;26(9):2282-94.

Table 1: Frequent and Novel Variants

Variant (HGVS)*		Patients	Pedigrees	Patients	Pedigrees
c.DNA	Protein	(n=)	(n=)	(%)	(%)
Frequent Variants					
c.304C>T	p.(Arg102Trp)	10	10	7.6%	7.9%
c.574C>T	p.(Pro192Ser)	8	8	6.1%	6.3%
c.214G>A	p.(Glu72Lys)	8	7	6.1%	5.6%
c.598C>T	p.(Arg200Cys)	7	7	5.3%	5.6%
c.35T>A†	p.(Leu12His)	6	6	4.5%	4.8%
c.421C>T	p.(Arg141Cys)	5	5	3.8%	4.0%
c.(?_1-1)_(52+1_53-1)del	p.(=)	4	4	3.0%	3.2%
c.305G>A	p.(Arg102Gln)	8	4	6.1%	3.2%
c.579dup	p.(Ile194Hisfs*70)	4	4	3.0%	3.2%
c.589C>T	p.(Arg197Cys)	3	3	2.3%	2.4%
c.637C>T	p.(Arg213Trp)	3	3	2.3%	2.4%
c.78G>C	p.(Glu26Asp)	3	3	2.3%	2.4%
Novel Variants					
c.20del	p.Gly7Alafs*119	1	1	0.8%	0.8%
c.185-1G>A	p.(=)	1	1	0.8%	0.8%
c.336_337delinsTT	p.Trp112_Leu113delinsCysPhe	1	1	0.8%	0.8%
c.378del	p.Leu127*	2	2	1.5%	1.6%
c.435dup	p.Ile146AsnfsTer15	1	1	0.8%	0.8%
c.515del	p.Asn172Thrfs*65	1	1	0.8%	0.8%
c.574_580delinsACCCCCCT	p.Pro192Thrfs*72	1	1	0.8%	0.8%

* Sequence variant nomenclature was obtained according to the guidelines of the Human Genome Variation Society (HGVS) by using Mutalyzer (https://mutalyzer.nl/).
† In three patients from three different families the variant c.35T>A was in cis with the variant c.52+5G>C.

Table 2: Clinical Findings

Parameter	Mean ± SD, range, median
Age of Disease Onset (n=61)	16.5 ± 15.4, 0-58, 11 years
Common Symptoms and Findings at Presentation (n=75)	n= , %
Reduced BCVA	75 (100%)
Nyctalopia	6 (8.5%)
Strabismus	6 (8.5%)
Vitreous Haemorrhage	8 (7.2%)
Retinal Detachment	8 (7.2%)
Vitreous Haemorrhage and Retinal Detachment	6 (5.6%)
Nystagmus	1 (1.4%)
Fundoscopy Findings (n=108)	
Bilateral Findings	104 (96.3%)
Unilateral Findings	4 (3.7%)
Macular Schisis	89 (82.4%)
Peripheral Schisis	42 (38.9%)
Macular Atrophy	12 (11.1%)
Normal Fundus	4 (3.7%)

BCVA; best corrected visual acuity

Precis

This single-center consecutive, retrospective, observational study of molecularly confirmed adults and children, reports early disease onset, slow (often limited) progression, and diverse phenotypic features on fundus autofluorescence and optical coherence tomography.

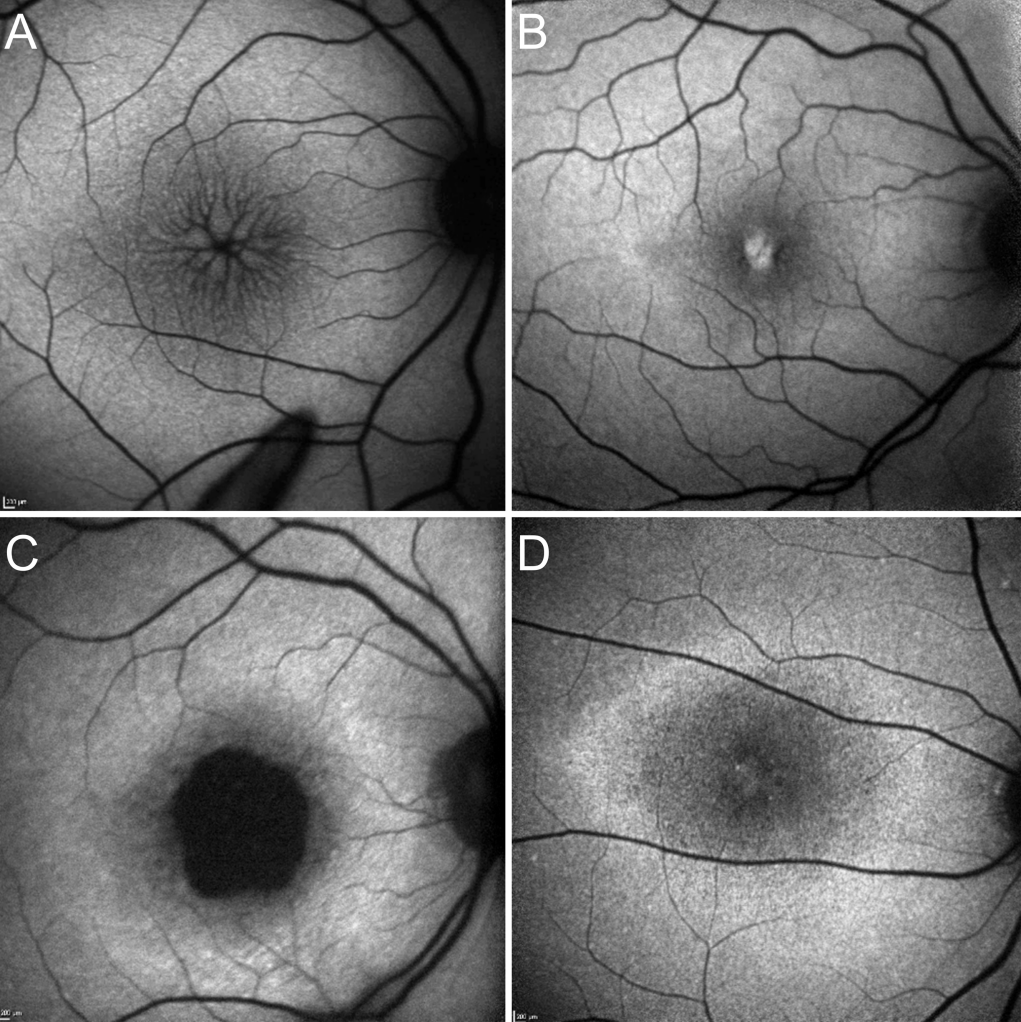
A
B
C
D

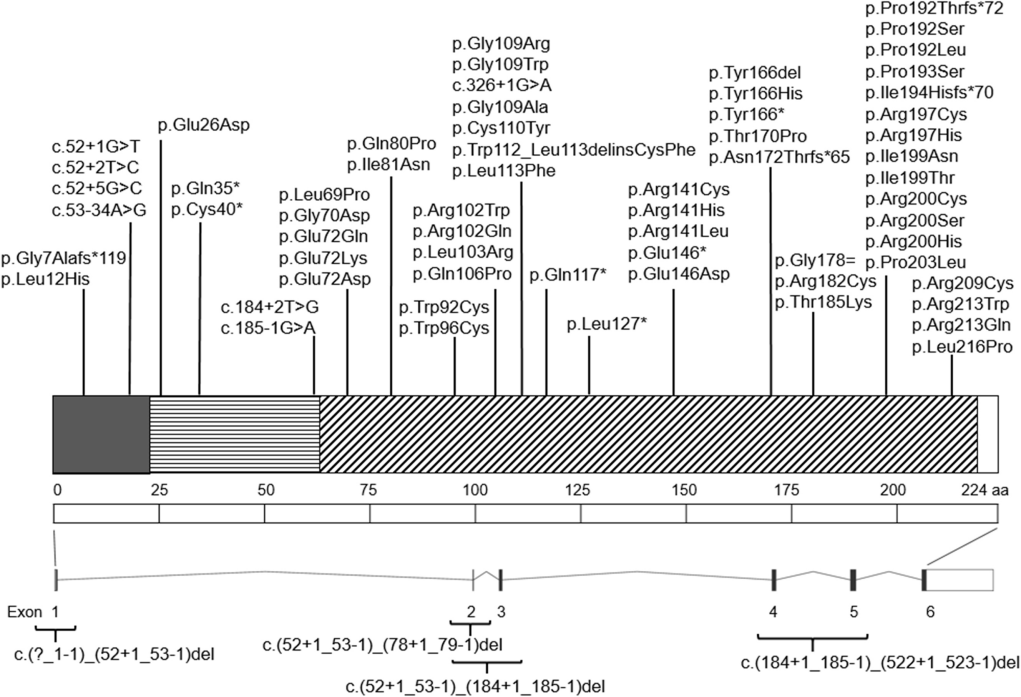
p.Gly7Alafs*119
p.Leu12His
c.52+1G>T
c.52+2T>C
c.52+5G>C
c.53-34A>G
p.Glu26Asp
p.Gln35*
p.Cys40*
c.184+2T>G
c.185-1G>A
p.Leu69Pro
p.Gly70Asp
p.Glu72Gln
p.Glu72Lys
p.Glu72Asp
p.Gln80Pro
p.Ile81Asn
p.Arg102Trp
p.Arg102Gln
p.Leu103Arg
p.Gln106Pro
p.Trp92Cys
p.Trp96Cys
p.Gly109Arg
p.Gly109Trp
c.326+1G>A
p.Gly109Ala
p.Cys110Tyr
p.Trp112_Leu113delinsCysPhe
p.Leu113Phe
p.Gln117*
p.Leu127*
p.Arg141Cys
p.Arg141His
p.Arg141Leu
p.Glu146*
p.Glu146Asp
p.Tyr166del
p.Tyr166His
p.Tyr166*
p.Thr170Pro
p.Asn172Thrfs*65
p.Gly178=
p.Arg182Cys
p.Thr185Lys
p.Pro192Thrfs*72
p.Pro192Ser
p.Pro192Leu
p.Pro193Ser
p.Ile194Hisfs*70
p.Arg197Cys
p.Arg197His
p.Ile199Asn
p.Ile199Thr
p.Arg200Cys
p.Arg200Ser
p.Arg200His
p.Pro203Leu
p.Arg209Cys
p.Arg213Trp
p.Arg213Gln
p.Leu216Pro
0
25
50
75
100
125
150
175
200
224 aa
Exon 1
2
3
4
5
6
c.(?_1-1)_(52+1_53-1)del
c.(52+1_53-1)_(78+1_79-1)del
c.(52+1_53-1)_(184+1_185-1)del
c.(184+1_185-1)_(522+1_523-1)del

A

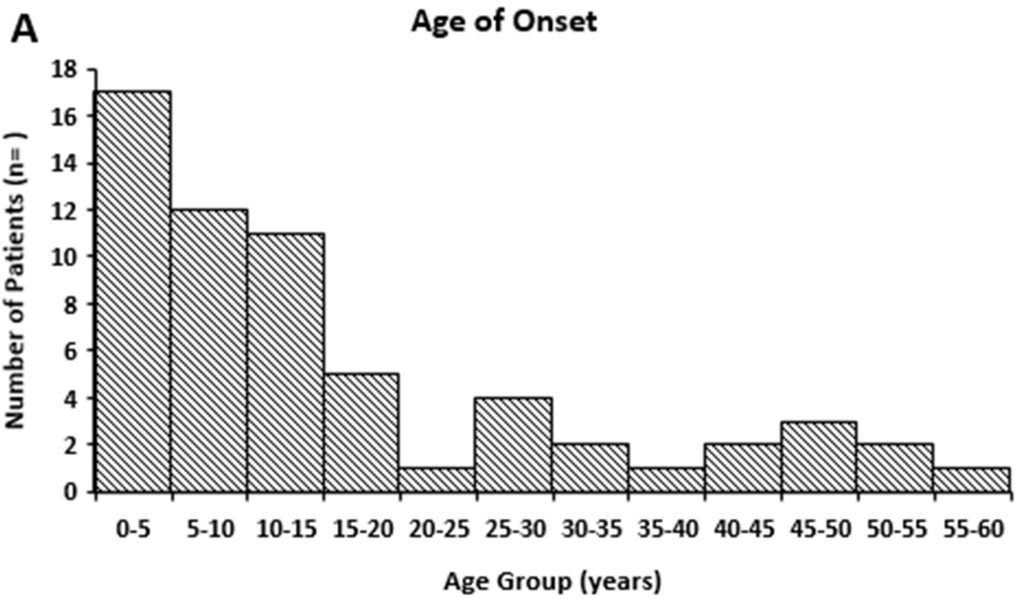
Age of Onset
Number of Patients (n=)
18
16
14
12
10
8
6
4
2
0
0-5
5-10
10-15
15-20
20-25
25-30
30-35
35-40
40-45
45-50
50-55
55-60
Age Group (years)

B

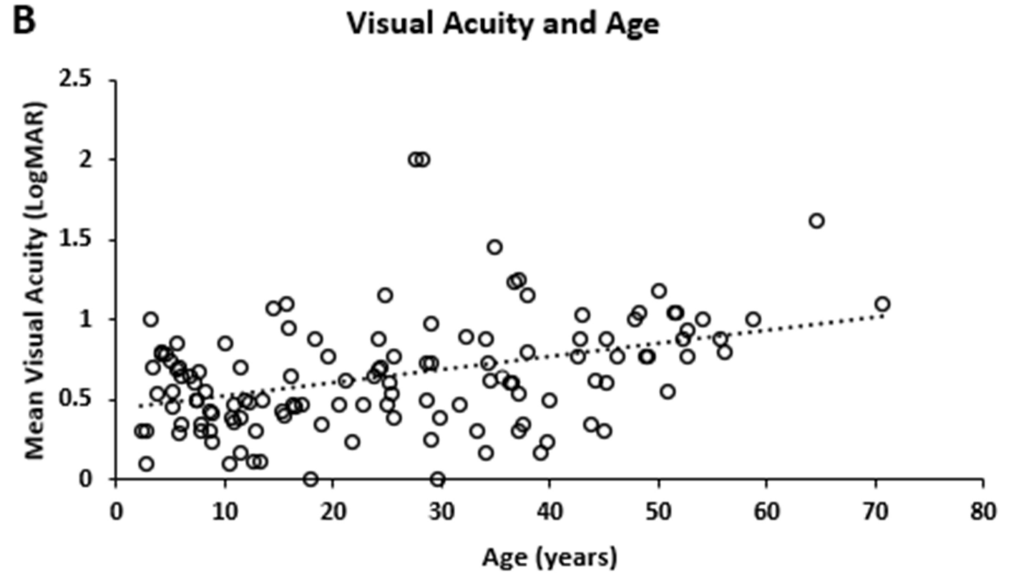
Visual Acuity and Age
Mean Visual Acuity (LogMAR)
2.5
2
1.5
1
0.5
0
0
10
20
30
40
50
60
70
80
Age (years)